A PHENOMENOLOGICAL MODEL TO INVESTIGATE EXCITONIC EFFECTS ON PHOTOLUMINESCENCE INTENSITY OF NANOSILICON

SUBMITTED IN PARTIAL FULFILMENT OF THE
REQUIREMENTS FOR THE DEGREE OF
MASTER OF SCIENCE IN PHYSICS
AT
ADDIS ABABA UNIVERSITY
ADDIS ABABA, ETHIOPIA
JUNE 2009

By

Tesfaye Shiferaw Haile

ADDIS ABABA UNIVERSITY
DEPARTMENT OF
PHYSICS

The undersigned hereby certify that they have read and recommend to the School of Graduate Studies for acceptance a thesis entitled "**A phenomenological model to investigate excitonic effects on photoluminescence intensity of nanosilicon**" by ***Tesfaye Shiferaw Haile*** in partial fulfilment of the requirements for the degree of **Master of Science in Physics**.

Dated: June 2009

Advisor: _____
Dr. S. K. Ghoshal

Examiners: _____
Dr. Mulugeta Bekele

_____
Prof. Malnev V.

ADDIS ABABA UNIVERSITY

Date: **June 2009**

Author: ***Tesfaye Shiferaw Haile***

Title: **A phenomenological model to investigate excitonic effects on photoluminescence intensity of nanosilicon**

Department: **Physics**

Degree: **M.Sc.** Convocation: **July** Year: **2009**

Signature of Author

To my beloved father Shiferaw Haile.

Table of Contents

List of Tables

List of Figures

Acknowledgements

I would like to thank Dr. Sib Krishna Ghoshal, my advisor and instructor, for his many valuable suggestions and constant support during the study.

I would also like to express my great gratitude to my family especially, to Mr. Workie Zewdu for his remarkable support and motivation.

Finally, I would like to mention that my graduate study was sponsored by Dire Dawa University.

Tesfaye Shiferaw Haile

June, 2009

Abstract

Visible photoluminescence from nano-silicon is one of the most attractive and debatable issue in recent years. Studying photoluminescence and understanding its mechanism has tremendous attention due to optoelectronic applications. When the size of quantum dots decreases the surface area to volume ratio increases and localized surface states appears in the forbidden region. Exciton energy states are also exists in the same gap region. It is important to examine the combined effects of exciton, localized surface states and quantum confinement effects. We have explicitly integrated these effects in a phenomenological model to obtain analytical expression for the photoluminescence spectra. Initially, we explicitly calculated the exciton binding energy and we incorporate the exciton contribution then combined it with quantum confinement model and surface states to see its effect on photoluminescence. Accordingly, we observed that taking the effect of exciton states into account explains almost accurately the experimental photoluminescence data. The results obtained using MATLAB programming. Calculations take place at room temperature on small quantum dots (1 - 5 nm). In conclusion, our results are quite new and it reflect some of the feature that has quite close correspondence with the experimental. The results are also in conformity with other theoretical and experimental investigations.

Chapter 1

Introduction

Silicon is the most widespread semiconductor in modern microelectronics technologies [1]. Its natural abundance, low cost, and high purity, as well as the high electronic quality of the Si/SiO_2 interface, have led to its overcoming dominance in microelectronic devices. Still, the use of silicon in optoelectronics remains highly limited. This state of affairs has remained, in fact, almost unchanged because of a fundamental property of the silicon band structure, 'indirect band gap' as shown in figure 1.1. The indirect radiative inter-band transitions in bulk silicon strongly inhibited because an emitted photon cannot satisfy the momentum conservation law for transitions from the conduction band minimum to the top of the valence band. The photon wave vector is about three orders of magnitude less than that required for the transition between the conduction band minimum and valence band maximum. This difference in **k**-space is $k_\Delta = 0.86 \times 2\pi/a$ [2], with a being the lattice constant of silicon, equal to 5.43 $\mathring{A}$. The electron-hole radiative recombination in the bulk material has forbidden unless additional mechanisms make the momentum conserved by relating the recombination process. The most probable means to have a radiative indirect transition without breakdown of the momentum conservation law is via phonon absorption or emission. However the electron-phonon interaction is weak; consequently, phonon assistance is a low-probability (and hence slow) process. This leads to a substantial increase of the total recombination time, and a decrease of the recombination probability compared to the direct radiative transitions in direct gap semiconductors.

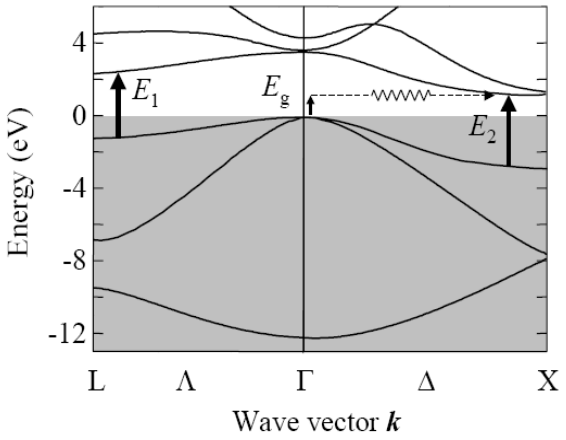

Figure 1.1: *Band structure of bulk silicon.*

The discovery of visible-range emission from nanocrystalline [3] in the early 1990s suggested that some of the problems associated with the silicon band structure might be overcome in nanoscale crystallites hosted in a wide-gap dielectric matrix like SiO_2, in order to create a strong confining potential for carriers inside the nanocrystal. Electronic states localized within the nanocrystal and the momentum distribution spreads due to the Heisenberg uncertainty relations. In other words, the wave functions consist of plane waves with all possible wave vectors including both $k \sim k_\Delta$ for holes and $k \sim 0$ for electrons, respectively. Thus, the momentum conservation law not violated in this case, which yields a nonzero probability of the direct radiative transition even in the absence of phonons.

1.1 Energy quantization and band gap of silicon quantum dot

A nanocrystal is a crystal with at least one dimension measured in nanometer scale. Nanoparticles are of great scientific interest as they are effectively a bridge between bulk materials and atomic or molecular structures [1]. Bulk materials have size independent physical properties whereas nanomaterials show strong size dependence on

their optical, electronic and thermodynamic properties. This is due to quantum confinement, hence quantum dots (QDs) obtains a very high surface area to volume ratio. One of the most important features of low-dimensional semiconductor structures is the confinement driven quantization of energy spectrum of charge carriers. The effect of quantum confinement becomes stronger as the confinement dimension increases and the size of a structure decreases. While bulk materials have a three-dimensional energy band structure, one-dimensional confinement of quantum wells leads to a two-dimensional energy band structure near each quantized energy level in the well and two-dimensional confinement of quantum wires leads to a one-dimensional energy band structure near each quantized energy level in the wire. On the other hand, three-dimensional confinement in quantum dots lead to a discrete (atomic-like) lower part of the energy spectrum [4]. The quantum confinement in different directions also changes wave functions describing the behavior of electrons and holes. As a result, the number of states per unit energy, the density of states, changes as a function of energy E of the particles shown in figure 1.2.

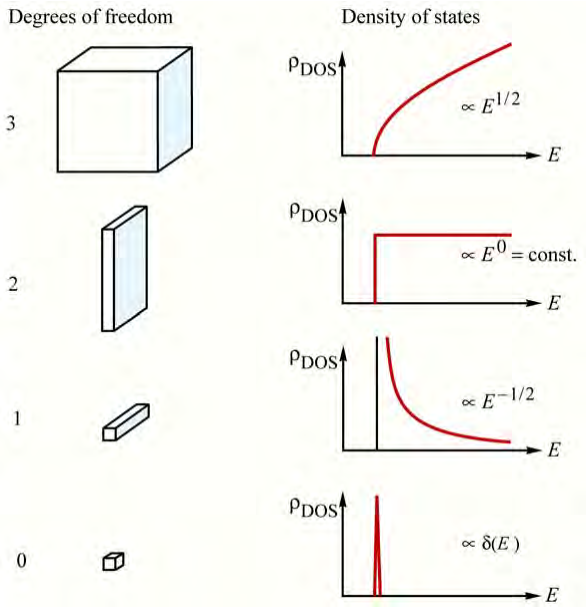

Figure 1.2: *Electronic density of states of semiconductors with 3, 2, 1 and 0 degrees of freedom for electron propagation. 2, 1 and 0 degrees of freedom referred to as quantum wells, quantum wires and quantum dots respectively.*

Generally, the density of states depends on the dimension of the nano-structure and the corresponding wave dispersion relation.

A particle behaves as if it were free when the confining dimension is large compared to the wavelength of the particle. During this state, band gap remains at its original energy due to continuous energy state. However, as the confining dimension decreases and reaches a certain limit, typically in nanoscale, the energy spectrum turns to discrete. As a result, band gap becomes size dependent. Specifically, the effect describes the phenomenon results from electrons and holes being squeeze into a dimension that approaches a critical quantum measurement, called the exciton Bohr radius. In addition to the quantum confinement, lattice contractions and surface passivation can also alter the band-gap of a material. Several models have proposed in order to describe band structure of semiconductors. Among those different models, effective mass approximation (EMA) is the simplest model which describes the band-gap of nanostructures specially quantum dots. Hence, the simplest model of an infinitely strong confining potential (i.e. infinitely high potential barriers at the dot boundary) it is possible to estimate the energies of electrons and holes localized inside the nanocrystal as proportional to R^{-2}, where R is the nanocrystal radius. Thus, the optical gap is

$$E_g(R) = E_g^{bulk} + \frac{A}{R^2} \tag{1.1.1}$$

where A is some positive constant, and A/R^2 represents the total energy of the non-interacting electron-hole pairs inside the dot.

However, as different experiments shows; when the size of nanocrystals decreases the optical band gap shift to the blue rang of visible spectrum, this blue-shift energy determined from such experiments, did not obey the law A/R^2 following from the simplest quantum-mechanical model. The dependence is rather $\sim R^{-\gamma}$ [5]. Figure 1.3 shows such dependence.

Therefore, after careful observations and calculations researchers expressed the optical band gap of quantum dot according to quantum confinement model as

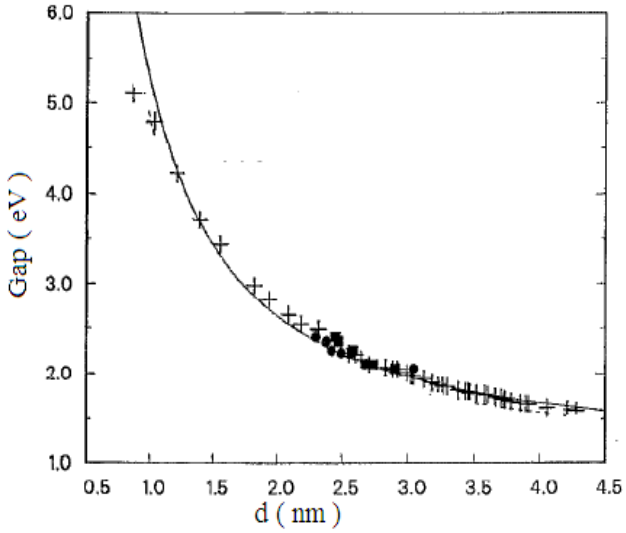

Figure 1.3: *Calculated optical band gap energies for various silicon crystal with respective to their diameter d (crosses). The continuous line is an interpolation and an extrapolation of these results by a* $d^{-1.39}$ *law [5].*

$$E_g^{QD} = E_g^{bulk} + \frac{\beta}{d^{\gamma}} \tag{1.1.2}$$

where d is diameter of quantum dots, where as β and γ are quantum confinement parameters.

1.2 Excitons and photoluminescence from silicon quantum dot

When an excitation takes place in a semiconductor by absorbing a photon a bound electron-hole state, exciton, is created. It is the overlap of wavefunctions that describes an electron and a hole. In fact, free electron and free hole are created whenever a photon of energy greater than the energy gap is absorbed in a crystal. The threshold for this process is $h\nu \geq E_g$ in a direct process. However, in the case of indirect band phonon-assisted process is takes place, at this time the threshold is

lower by the phonon energy $\hbar\Omega$. Excitons can be formed by photon absorption at any critical point $\nabla_{\mathbf{k}}(\epsilon_c(\mathbf{k}) - \epsilon_v(\mathbf{k})) = 0$. For bulk crystals, the electron-hole pair treated like hydrogen atom. The exciton energy levels appear just below the minima of conduction band, as shown in figure 1.4 [4].

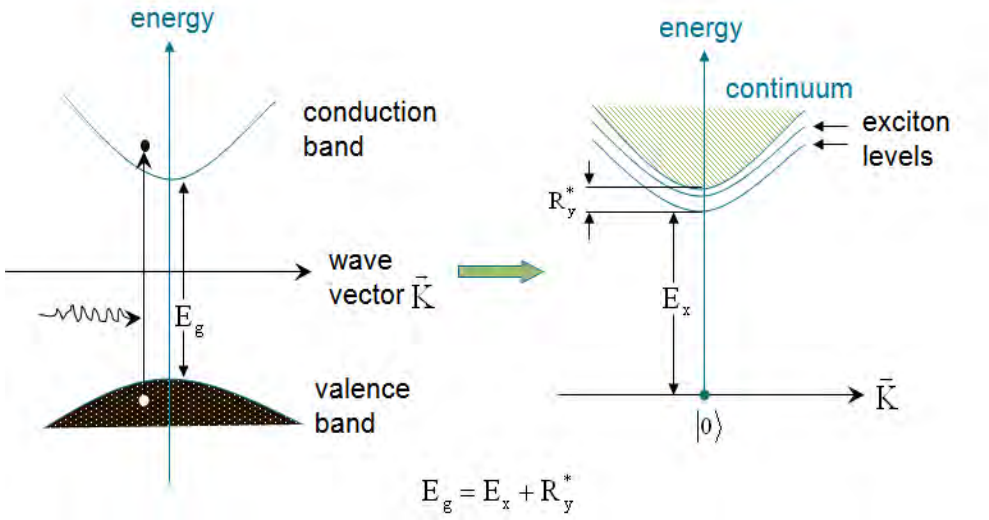

Figure 1.4: *Excitons energy levels.*

However, for small quantum dots, the electrons and the holes are in close proximity. Hence, the exciton energy states are described by solving the quantum mechanical problem of a particle in 3D box. Or the bound electron-hole states can be calculated by solving the schrodinger equation for particles (electrons and holes) with effective mass m_i^*, as well as a mutual interaction potential given by inter-particle spacing and affected by shielding due to the finite polarizability of the material, since as the dot size becomes smaller than exciton Bohr radius, $R < a_B$, the quantum confinement effect dominates.

Photoluminescence (PL) is a process in which a substance absorbs photons (Electromagnetic radiation) and then re-radiates photons. Quantum mechanically, this can be described as an excitation to a higher energy state and then a return to a lower energy state accompanied by the emission of a photon. In other word, it is the emission of light beam from semiconductors mainly when electrons and holes recombine i.e. when the wavefunction describing an electron and hole overlaps. When electrons

in the valance band exposed to a high-powered laser they will leave their orbits until the average energy drops to the bottom of the conduction band. Usually at this stage attraction of the holes overcomes the electrons and they recombine at the same time emits photons of energy equal to band gap energy. The recombination shows up as a peak on the emission spectrum usually at the band gap energy.

In general, as researchers found out silicon nanocrystals are capable of emitting electromagnetic energy in the visible spectrum, for instance; S. Tripathy *et al.* [6] studied the photoluminescence spectra from silicon nanocrystallites grown by pulsed plasma technique on quartz substrates and the photoluminescence spectra is shown in figure 1.5.

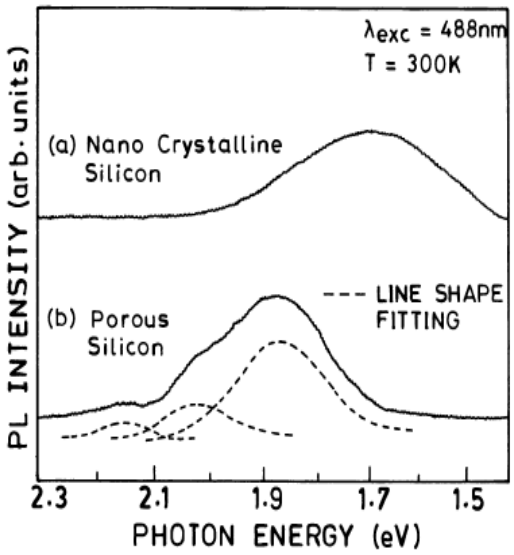

Figure 1.5: *Room temperature Raman spectra of (a) nanocrystalline silicon prepared by pulsed plasma processing and (b) porous silicon prepared by anodic etching using 488 nm line of Ar^+ laser [6].*

This is in contrast with bulk silicon, in which energy of inter-band transition corresponds to the band gap energy of 1.12 eV. In other word, energies of the emitted photons increases as the nanocrystal size decreases. Such an increase in optical band gap usually called a 'blue-shift' because the photon energy shifts toward the shorter wavelength side of the visible spectrum.

1.3 Quantum efficiency

The indirect band structure of bulk silicon leads a low probability for radiative recombination, which in turn means that the e-h radiative lifetime is long (of the order of some milliseconds). An e-h pair has to wait on average a few milliseconds to recombine radiatively. During this time, both the electron and the hole move around and cover a volume of the order of 10 μm^3 [11]. If they encounter a defect or a trapping center, the carriers might recombine nonradiatively. Typical non-radiative recombination lifetimes in bulk silicon are of the order of some nanoseconds. Thus, the internal quantum efficiency

$$\eta = \Gamma_{rad}/(\Gamma_{rad} + \Gamma_{nr})$$

Where Γ_{rad} *and* Γ_{nr} are the probability for radiative and non-radiative recombination rates respectively, is the measure for the probability of the total de-excitation, which radiatively recombined; is about 10^{-6}. This is the reason why bulk silicon is a poor luminescent material. Many strategies have explored over the years to overcome this limitation and some of them have based on the spatial confinement of the carriers, others on the introduction of impurities, the use of quantum confinement, and the use of Si-Ge alloys or super-lattices. It is known that the indirect band structure of bulk silicon changed to direct when the dimension reaches a few nanometer scale. At this time the probability for radiative recombination, get over the non-radiative one. On the other hand, the confinements of e-h pair in real space leads to a spread of the wave function in the reciprocal space and then radiative recombination can occur in a first-order process [12]. The radiative recombination time τ of a first - order radiative process defined from the Fermi golden rule as

$$\frac{1}{\tau} = \frac{16\pi^2}{3}\frac{ne^2}{h^2m^2c^3}E_o \mid \langle i_{BC} \mid p \mid f_{BV} \rangle \mid^2$$

Where $\mid i_{BC}\rangle$ is the initial state of the electron in the conduction band and $\mid f_{BV}\rangle$ is the final state in the valance band (i.e. the hole state). E_o is the energy of the transition and n is the refractive index of porous silicon. In the case of crystallites, the above equation takes into account the 3D confinements of an exciton. In strong

confinement regime ($R \leq a_B$), the wave function of the exciton is well approximated by the product $\mid i_{BC}\rangle \mid f_{BV}\rangle$.

1.4 Linear optical properties of silicon quantum dot

Optical absorption coefficient (α), oscillator strength (f) and dielectric function (ϵ) are some of linear optical properties of silicon quantum dots. The direct optical absorption coefficient (α) is proportional to the number of optical transitions per volume and time elements [7]. The coefficient calculated from simple optical principles and it is given by the absorbed energy per unit time and volume divided by the absorbed energy per unit time and volume divided by the energy flux $2\pi A_o^2 \nu^2 \varepsilon_o n_r/c$, where A_o and n_r are the amplitude of absorbed light and refractive index of silicon nanocrystallites. The energy flux is equal to optical energy density given by the square of the wave amplitude per wavelength interval, $2\pi A_o^2 \nu^2 \varepsilon_o n_r^2/c^2$ divided by the light velocity in the quantum dots c/n_r.

The optical properties of an ordered arrangement of nanocrystallites are evaluated within the independent-particle approximation and using the Bloch representation of the artificial supercell, the composite medium of nanocrystals and vacuum, crystal. The imaginary part of the dielectric function (α = x,y,z) [8]

$$Im\ \epsilon_{\alpha\alpha}(\omega) = \frac{(2\pi e\hbar)^2}{m\Omega_o}\frac{1}{N}\sum_{\mathbf{k}}\sum_{c,v}\frac{f_{cv}^{\alpha\alpha}(\mathbf{k})}{E_c(\mathbf{k}) - E_v(\mathbf{k})}\delta(E_c(\mathbf{k}) - E_v(\mathbf{k}) - \hbar\omega) \qquad (1.4.1)$$

$$f_{cv}^{\alpha\alpha}(\mathbf{k}) = \frac{2m \mid \langle c\mathbf{k} \mid v_\alpha \mid v\mathbf{k}\rangle \mid^2}{E_c(\mathbf{k}) - E_v(\mathbf{k})} \qquad (1.4.2)$$

contains optical transitions between valence ($|v\mathbf{k}\rangle$) and conduction ($|c\mathbf{k}\rangle$) band states with the oscillator strengths $f_{cv}^{\alpha\alpha}(\mathbf{k})$ taken at N $\mathbf{k}$-points in the Brillouin zone (BZ). Ω_o is the volume of the supercell. Interestingly, the luminescence intensity is related to the absorption coefficient through an energy balance relation as long as the structures of the nanocrystallites have not changed in the excited state.

The nanocrystal size influences not only the energetical positions of the optical transitions but also their oscillator strengths. This clearly demonstrated in Fig. 1.6.

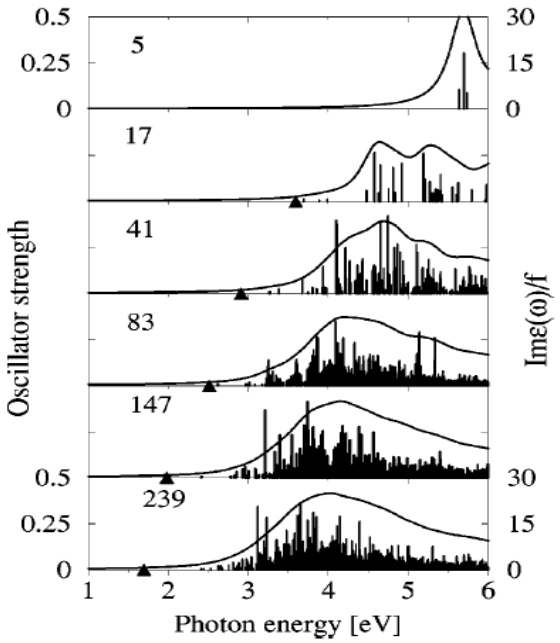

Figure 1.6: *Oscillator strengths of the optical transitions (vertical lines) versus the transition energies for Si crystallites with varying size. The normalized absorption spectrum Im $\epsilon(\omega)/f$ (solid line) is plotted to envelope the oscillator strengths. The number of atoms indicated for each crystallite. A triangle indicates the HOMO-LUMO gap [9].*

It presents the optical transitions at the center of the irreducible part of the Brillouin zone. The oscillator strengths $f_{cv}^{\alpha\alpha}(\mathbf{k})$, a measure of the relative strength of the electronic and/or optical transitions, calculated according to eqn. 1.4.2 plotted as vertical lines against the transition energies. It is particularly useful as a method of comparing transition strengths between different types of quantum mechanical systems. Figures 1.6 clearly show the quantum size effects on the electronic wave functions. Silicon nanocrystals with diameters above 1.5 nm a tail of weak transitions appears just above the HOMO-LUMO gap. The oscillator strengths of these transitions are much smaller than the maximum oscillator strengths of about 0.4. The occurrence of the tail can be interpreted as an indication of the development of bulk properties with increasing nanocrystal size.

1.5 Nonlinear optical properties of silicon quantum dot

Recently, in addition to the study of linear optical properties, a nonlinear optical property of silicon quantum dot attracts researchers' interest for photonic device applications, particularly in all-optical switching. Peoples have reported enhanced optical nonlinearity for porous silicon at different wavelengths. The third order nonlinear effects are generally characterized by nonlinear absorption β and nonlinear refractive index n_2 and described by

$$\alpha(I) = \alpha_o + \beta I$$

and

$$n(I) = n_o + n_2(I)$$

Where α_o and n_o stands for linear absorption and refractive index respectively. The β and n_2 values are used to evaluate the imaginary $Im\ (\chi^{(3)})$ and real $Re\ (\chi^{(3)})$ parts of the third order nonlinear susceptibility. Hence, its real part is obtained from

$$Re\ (\chi^{(3)}) = 2n_o^2 \varepsilon_o c n_2$$

Where ε_o is the permittivity of free space and c is velocity of light whereas the effective refractive index n_o is obtained to be 1.7.

Intensity dependent changes in optical properties like refractive index, third-order nonlinear susceptibility (shown in Fig. 1.7), and nonlinear absorption are the prominent ones.

It is observed through the z-scan technique that the real part of the third order nonlinear optical susceptibility $Re\ (\chi^{(3)}) \approx 1.4 \times 10^{-9} esu$ is of the order of magnitude higher than the corresponding imaginary part $Im\ (\chi^{(3)}) \approx 0.7 \times 10^{-10} esu$. This indicates that the nonlinearity is mostly refractive. The absolute value of $\chi^{(3)}$ is significantly larger than the bulk Silicon value $\sim 6.0 \times 10^{-12} esu$ [10]. This enhancement of $\chi^{(3)}$ in the case of low-dimensional structures is attributed to various mechanisms, but the

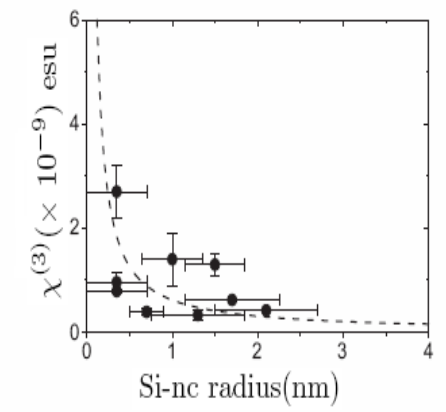

Figure 1.7: *The variation of $\chi^{(3)}$ with silicon nanocrystals (quantum dots) radius (R). The solid dots are experimental data and the dashed curve is the theoretical fit.*

effect of quantum confinement is the main reason for such enhancement. The higher values of nonlinear absorption in silicon quantum dots compared to that of crystalline bulk silicon are due to either multi-photon absorption or saturation of single-photon absorption.

1.6 Silicon quantum dot for photonic applications

The aim of recent investigations are towards the development of photonic applications in which multi-layer porous silicon structures are used to fabricate Bragg reflectors, Fabry-Perot filters and micro-cavities [10]. The fabrication and optical characterization of dielectric porous silicon multi-layers with periodic variation of refractive index as a function of depth is possible through etch process. These complex multi-layers structures have used to create interferential filters and/or narrow band reflectors formed by dielectric films. Bragg reflectors and Fabry-Perot devices fabricate on the bases of these multi-layers that help to tune and narrow down the p-emission band. Other application of porous silicon multi-layers includes planer wave-guides in infrared and visible region. Commercial application presently hindered by scattering loss and absorption in the porous medium.

The Fabry-Perot devices help to fabricate porous silicon micro-cavities, which act as confinement region for emitted photons and modify the photon density of states

that finally lead to alterations of spontaneous emission characteristics. The effect of micro-cavity manifested in many ways: (i) A 16-fold increase in intensity, (ii) Strong narrowing of emission band, (iii) Decrease in the luminescence decay time constant, and (iv) Strong directional emission from the micro-cavity. These features are evidence through angular resolved photoluminescence measurements and time-resolved excitation spectroscopy.

Porous silicon Schottky diodes have studied with yielding efficiencies 10^{-4}. These types of diodes are use to achieve porous silicon light emitting diodes (LEDs) with improved performance. The current voltage characteristics proved to be independent of the type of metal used for the electrical contact. Devices based on Si homo-junctions have fabricated for providing more adequate carrier injection mechanism for efficient electroluminescence (EL) and slower degradation. Micro-cavity LEDs are very useful to achieve efficient EL. In 1996 attempt was made to integrate a porous silicon LED with Si electronics and it was possible to turn the LED on and off by applying small current pulse to the base of the transistor. Finally, arrays of such integrated structures fabricated.

The very large value of the surface to volume ratio for sponge porous structures of Si $500m^2cm^{-3}$ makes them highly chemically reactive. This feature of porous silicon exploited for sensors applications to sense humidity, organic molecules, ethanol, nitrous oxide etc. Biosensors based on porous silicon micro-cavities are very useful for distinguishing bacteria and viruses because these cavities have strong response to DNA molecules and lipids. Through parametric distinction of physical properties (integrated PL as sensing parameter, refractive, and PL peak) such biosensors are used to measure concentration of polar species.

Nano-silicon is a good candidate for developing two-dimensional photonic crystals (2D-PC) by anodic electrochemical dissolution method. This method is technologically friendly, simpler, cheaper, and faster and wafer scalable. These 2D-PC made from porous silicon has air columns in the Si-matrix that acts as macro-pores. They can fill with active materials to form either enhanced LEDs or nonlinear media. Another application of porous silicon is in fabricating porous silicon Fibonacci quasi-crystals. In these structures, the localization of light waves helps for many nonlinear

applications. Researchers observed that the electric field intensity of optical modes shows local field enhancement effect, which is due to the weak localization of modes. This investigation is very important from fundamental physics point of view as the time resolved propagation measurements on porous silicon Fibonacci quasi-crystals demonstrate the presence of localized photon states.

1.7 Thesis objectives

In this research work, our main aim is to calculate exciton binding energy and see its effect on optical band gap and photoluminescence spectra of small sized silicon quantum dots.

Specifically, we devote

⇛ to derive an expression for exciton binding energy using effective mass approximation and quantum confinement model together.

⇛ to derive an expression for optical band gap by taking exciton energy states in the band gap into account.

⇛ to derive an expression for photoluminescence intensity by taking exciton and surface states into account.

⇛ to generate photoluminescence spectra by considering exciton states, discuss our results, after that summarize, and conclude our study.

1.8 Thesis outline

Based on our objectives, in this research work, we analyze the influence of exciton binding energy on photoluminescence spectra and photoluminescence peak of silicon quantum dots by integrating surface states and quantum confinement model to explain experimental data.

The thesis organized in to five Chapters. In chapter 2, we deduce the exciton binding energies of excitons in silicon quantum dots using effective mass approximation together with quantum confinement model for two limiting cases based on the ratio of quantum dots and exciton Bohr radius. In chapter 3, we formulate a phenomenological model to generate photoluminescence spectra of silicon quantum dot by taking the existence of surface and exciton energy states in the band gap into account. In chapter 4, we report the results we obtained for optical band gap and photoluminescence spectra together with the experimental plot side by side in order to compare our results with the experimental data and we also explain our results and finally, we summarize and conclude our study in the fifth chapter.

Chapter 2

Calculation of exciton binding energy

Researchers have been tried to find out an expression that assures the position of lowest energy level of an exciton in a quantum dots. Therefore, in this chapter we are going to express the position of exciton energy states of silicon quantum dots using effective mass approximation and quantum confinement models, expression for exciton binding energy and other form of band gap dependencies on dot size by considering exciton states.

To do so, let us model the excitons in silicon quantum dot as particles in a spherical infinite potential well of radius R. That is, for energy $E > 0$ they move in simple central potential given by:

$$V(\mathbf{r}) = \begin{cases} o & \text{for } 0 \leq \mathbf{r} \leq R, \\ \infty & \text{otherwise.} \end{cases}$$

The wave function has known only non-zero in the region $0 \leq \mathbf{r} \leq R$. In this region, they are subject to the physical boundary conditions that they are well-behaved at $\mathbf{r} = 0$, and zero at $\mathbf{r} = R$. Writing the wave function in standard form

$$\psi(\mathbf{r}, \theta, \phi) = R_{n,l}(\mathbf{r}) Y_{l,m}(\theta, \phi)$$

The Hamiltonian of a particle in a spherical infinite well potential is

$$H = \frac{-\hbar^2}{2m}[\frac{\partial^2}{\partial r^2} + \frac{2}{r}\frac{\partial}{\partial r} - \frac{\hat{L}^2}{\hbar^2 r^2}] + V(r)$$

Therefore, the Schrodinger equation in the region $0 \leq \mathbf{r} \leq R$ is

$$\frac{-\hbar^2}{2m}[\frac{\partial^2}{\partial r^2} + \frac{2}{r}\frac{\partial}{\partial r} - \frac{\hat{L}^2}{\hbar^2 r^2}]\psi(\mathbf{r}, \theta, \phi) = E\psi(\mathbf{r}, \theta, \phi)$$

It implies that, the radial function $R_{n,l}(\mathbf{r})$ satisfies

$$\frac{d^2 R_{n,l}}{dr^2} + \frac{2}{r}\frac{dR_{n,l}}{dr} + (k^2 - \frac{l(l+1)}{r^2})R_{n,l} = 0$$

where

$$k^2 = \frac{2mE}{\hbar^2}$$

Defining the scaled radial variable $z = k\mathbf{r}$, the above differential equation can be transformed into the standard form

$$\frac{d^2 R_{n,l}}{dz^2} + \frac{2}{r}\frac{dR_{n,l}}{dz} + [1 - \frac{l(l+1)}{z^2}]R_{n,l} = 0$$

The two independent solutions to this well-known second-order differential equation are called *spherical Bessel function and spherical Neumann function* , and written as

$$j_l(z) = z^l(-\frac{1}{z}\frac{d}{dz})^l(\frac{\sin(z)}{z})$$

$$n_l(z) = -z^l(-\frac{1}{z}\frac{d}{dz})^l(\frac{\cos(z)}{z})$$

We knew that, the spherical Bessel functions are oscillatory in nature, passing through zero many times. However, the $n_l(z)$ functions are badly behaved (i.e., they are not square-integrable) at $z = 0$, whereas the $j_l(z)$ functions are well-behaved everywhere. It follows from our boundary condition at $r = 0$ that the $n_l(z)$ are unphysical, and that the radial wave-function $R_{n,l}$ is thus proportional to $j_l(z)$ only.

Taking the lowest allowed state $j_0(\mathbf{kr})$ and using the boundary condition that $j_0(\mathbf{k}R) = 0$, the lowest value of k is given by

$$k_{min}^2 = \frac{\pi^2}{R^2} \tag{2.0.1}$$

Therefore, the band gap of quantum dot will be

$$E_g^{QD} = \epsilon_c(k_{min}) - \epsilon_v(k_{min}) = \epsilon_c + \frac{\hbar^2}{2m_e^*}k_{min}^2 - (\epsilon_v - \frac{\hbar^2}{2m_h^*}k_{min}^2) = E_g^{bulk} + \frac{\hbar^2\pi^2}{2\mu R^2} \tag{2.0.2}$$

where ϵ_c, ϵ_v and μ are energy of the minima of conduction band, energy of the maxima of valance band and the reduced mass respectively, with

$$\frac{1}{\mu} = \frac{1}{m_e^*} + \frac{1}{m_h^*} \tag{2.0.3}$$

where $m_e^* \, and \, m_h^*$ are effective mass of electron and hole respectively. Here we assumed that effective mass of electron and holes are unaffected by finite size (many atoms in the nanocrystals).

We have two confinement limits for an exciton in quantum dots depending upon the ratio between the radius R of quantum dots and Bohr exciton radius a_B, i.e. when $R/a_B \gg 1$ and $R/a_B \leq 1$. Hence, we look at the energies of an exciton in each such liming case.

2.1 Energies of weakly confined excitons

When the radius of quantum dots much greater than Bohr exciton radius i.e. $R \gg a_B$ the exciton said to be weakly confined. In this confinement regime, the character of the exciton as a quasiparticle conserved well while the translational degrees of freedom are confined with little energy increments [14]. Therefore, for such confinement case the use of effective masses, center of mass motion and dielectric screening are a valid approximation but particle walls will have limited effect on exciton binding energy.

let us consider the Mott-Wannier excitons where electron and hole attracted to each other by Coulomb potential

$$V(r) = \frac{-e^2}{\varepsilon_r r} \tag{2.1.1}$$

where ε_r is the relative static permittivity and r the distance between electron and hole. This leads to the bound stats of the system with energies lower than the minima of conduction band. In bulk semiconductors, the problem is that of the hydrogen atom and the exciton states have energies given by the Rydberg equation

$$E_n = E_g - \frac{\mu e^4}{2\hbar^2 \varepsilon^2 n^2} \tag{2.1.2}$$

Therefore, in weakly confinement regime the Hamiltonian of the confined exciton given by

$$H = \frac{P_e^2}{2m_e^*} + \frac{P_h^2}{2m_h^*} - \frac{e^2}{\varepsilon \mid \mathbf{r_e} - \mathbf{r_h} \mid} \tag{2.1.3}$$

and the size dependent exciton energy is then given by

$$E_{nml} = E_g^{bulk} - \frac{E_{RY}^*}{n^2} + \frac{\hbar^2 \chi_{ml}^2}{2MR^2} \tag{2.1.4}$$

Actually, this exciton energy consists of contribution due to centrosymmetric Coulomb potential resulting in e-h binding and contribution due to the motion of the combined e-h state with total mass $M = m_e^* + m_h^*$ with an angular distribution given by quantum numbers m,l and χ_{ml} is the roots of the Bessel function. Therefore, the lowest energy state of the exciton found when $n = 1,\ m = 1\ and\ l = 0$ i.e. when $\chi_{ml} = \pi$ and it is expressed as

$$E_{1s1s} = E_g^{bulk} - E_{RY}^* + \frac{\hbar^2 \pi^2}{2MR^2} \tag{2.1.5}$$

On the other hand, it has written in terms of exciton Rydberg energy E_{RY}^*, energy difference between bound and unbound electron-hole pair, [15] as

$$E_{1s1s} = E_g^{bulk} - E_{RY}^*[1 - \frac{\mu}{M}(\frac{\pi a_B}{R})^2] \tag{2.1.6}$$

Note, this energy of an exciton in its lowest state is equally probable anywhere in the nanocrystal.

where E_{RY}^* is given by

$$E_{RY}^* = \frac{\mu}{m_o}\frac{1}{\varepsilon_r^2} \times 13.6eV$$

This energy contributes to all optical properties as a result quantum efficiency of nano-silicon enhances.

2.2 Energies of strongly confined excitons

When $R \leq a_B$ 'strong confinement regime', the exciton Bohr radius for silicon is $\sim$ **4.9** nm [13] which is a fairly small number among semiconductor quantum dots because of the relatively large effective mass of the charge carriers in silicon, the confinement

effect dominates and the electron and hole will be viewed as individual particles predominantly in their respective ground states with only little spacial correlation between them [14]. In this confinement regime, unlike to weakly confined exciton we can take the effect of confinement potential $V(\mathbf{r_e}, \mathbf{r_h})$ into account. Hence, the Hamiltonian of an exciton strongly confined in a quantum dot of radius R given by

$$H = \frac{P_e^2}{2m_e^*} + \frac{P_h^2}{2m_h^*} - \frac{e^2}{\varepsilon \mid \mathbf{r_e} - \mathbf{r_h} \mid} + V(\mathbf{r_e}, \mathbf{r_h}) \tag{2.2.1}$$

where $\mathbf{r_e}$ and $\mathbf{r_h}$ are the positions of the electron and hole respectively, and

$$V(\mathbf{r_e}, \mathbf{r_h}) = \begin{cases} o & \text{if } r_e, r_h < R, \\ \infty & \text{otherwise.} \end{cases}$$

Exciton binding energy follows from solving schrodinger equation by taking the confinement potential into account. So, the position of the lowest exciton energy state has expressed [16] as

$$E_{1s1s} = E_g^{bulk} + \frac{\pi^2\hbar^2}{2\mu R^2} - 1.786(\frac{a_B}{R})E_{RY}^* - 0.248E_{RY}^* \tag{2.2.2}$$

Where the second term corresponds to the sum of the single-particle ground state energies (kinetic energies), the third term to the Coulomb attraction and the last one for spatial correlation between the two particles.

On the other hand, using the band gap energy expression from eqn. 2.0.2 we find an alternative expression for the lowest exciton energy state as

$$E_{1s1s} = E_g^{QD} - 1.786(\frac{a_B}{R})E_{RY}^* - 0.248E_{RY}^* \tag{2.2.3}$$

From such expression, we understood that the exciton binding energy should be

$$E_b = 1.786(\frac{a_B}{R})E^*_{RY} + 0.248E^*_{RY} \tag{2.2.4}$$

The energy levels of bound electron-hole states will be affected by the dot size, since the wavefunctions of both the electron and the hole have been quantum confined.

Now, using the band gap energy from quantum confinement model (eqn. 1.2.2) we have obtained the following band gap expression, by taking the effects of exciton binding energy into account.

$$E_g^{QD'} = E_g^{bulk} + \frac{\beta}{d^\gamma} - 1.786(\frac{a_B}{R})E^*_{RY} - 0.248E^*_{RY} \tag{2.2.5}$$

We use this expression in the next chapter to drive an expression for the photoluminescence spectra. It is important to note that, no one has incorporated this contribution before to investigate the optical behavior. We believe that the photoluminescence peak originates from this and the shift in the photoluminescence peak may have some connection to this effect.

Chapter 3

Analytical treatment of photoluminescence intensity

Of all the forms of silicon containing quantum dots, porous silicon is the one that has attracted the most attention to date, mostly because of its intense visible photoluminescence. Numerous models have proposed to explain its photoluminescence, including quantum confinement, surface states, defects in the oxide, and even specific chemical species. Presently, although a detailed understanding of the photoluminescence has yet to be achieved, it is usually accepted that the band gap opens because of quantum confinement, which pushes the photoluminescence in to the visible region of light spectra for crystal sizes below 5 nm [17]. Therefore, in this chapter we are going to discuss effects of exciton energy states on photoluminescence peak and formulate a phenomenological model to obtain analytical expression for the photoluminescence spectra from silicon quantum dots.

3.1 Effect of surface states on photoluminescence

When the valence electrons $3s^2$ $3p^2$ of a silicon atom form hybrid orbitals sp^3 to make bonds with neighboring atoms, their energy levels split into bonding and anti-bonding states. The valence electrons have accommodated in the bonding state, so the anti-bonding state is empty. Since in a crystal many atoms make bonds with each other to arrange themselves periodically, these energy levels have broadened to make bands: the valence band and the conduction band, respectively. These are

electronic states in a bulk crystal. However, on the surface there exist dangling bonds (unpaired hybrid orbitals), which are similar to the hybrid orbitals of isolated atoms, whose energy levels will be located between the bonding and antibonding states, or within an energy gap see figure 3.1.

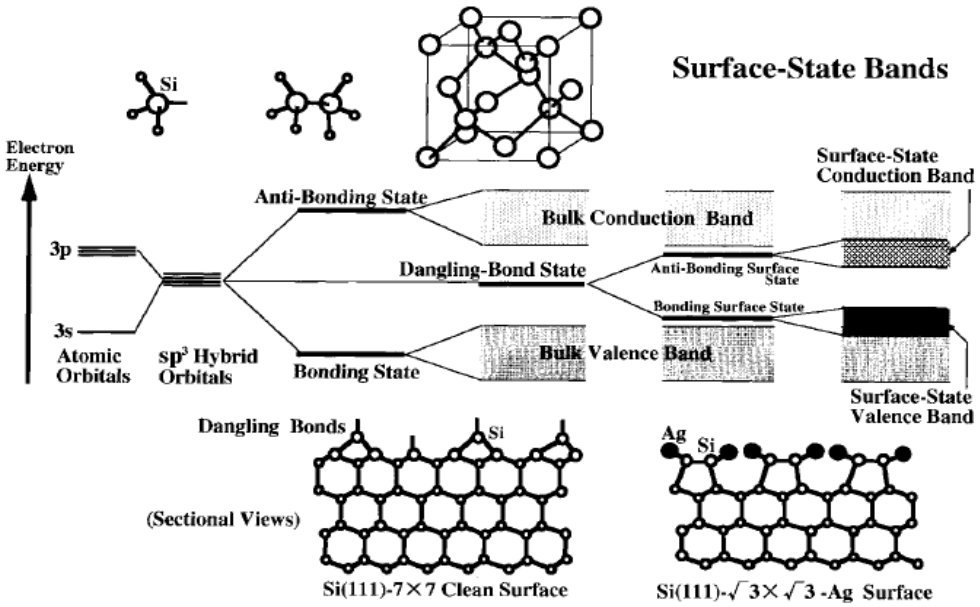

Figure 3.1: *A schematic energy diagram for atoms and molecules, and also the bulk and the surface of a silicon crystal.*

In fact, the dangling-bond states on a clean Si (111) surface lie around the middle of the band gap [18]. In addition, as mentioned in chapter one, surface to volume ratio increase as the crystal size decreases hence; the influence of surface states on the photoluminescence from smaller crystals will be highly enhanced. Therefore, the role of surface states, especially for low crystal size should be included into account during the study of photoluminescence mechanism.

Wolkin *et al.* [17] obtained photoluminescence spectra at room temperature by using a pulsed excitation nitrogen laser (337 nm) and/or a continuous excitation HeCd laser (325 nm).

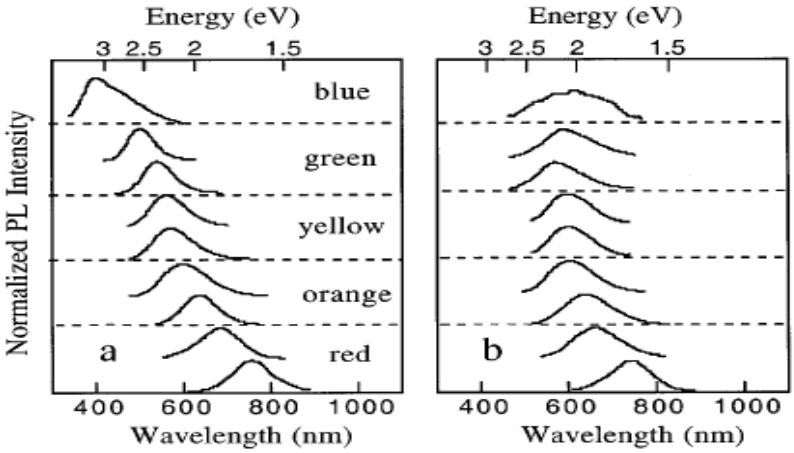

Figure 3.2: *Room temperature photoluminescence spectra from porus silicon samples with different porosities kept under Ar atmosphere (a) and after exposure to air (b).*

Accordingly, figure 3.2 (a) shows the photoluminescence spectra of five types of oxygen-free pours silicon samples with different porosities. Stable red, orange, yellow, green and blue spectra have observed as increasing the order of porosity. The results have obtained and measured during the samples kept in the Ar environment. Whereas, figure 3.2 (b) shows how the spectra were modified after the samples had been exposed to air for 24 h and they observed that oxidation introduces states in the band gap which pin the transition energies. In addition, below about 3 nm in size, oxide passivated nanocrystals are luminesce at lower energy than hydrogen passivated nanocrystals [19]. Calculation shows that the size of the band gap and the corresponding spatial pattern of the highest occupied molecular orbital (HOMO) and lowest unoccupied molecular orbital (LUMO), depend upon the electronegativity of the passivating layer at such small size. In oxide, terminated nanocrystals the HOMO is sketch to the surface and resides in weakened Si - Si back bonds on interfacial Si atoms directly bonded to oxygen.

Therefore, we realized that as the silicon exposed to air oxygen make a bond with the dangling bond and the SiO_2 layer cover the surface as shown in figure 3.3, the same is true when the dandling bond makes a bond with Hydrogen, and surface states appears in the band gap. Consequently, the photoluminescence peak shifted (modified) due to surface states. Therefore, surface passivation has remarkable effect

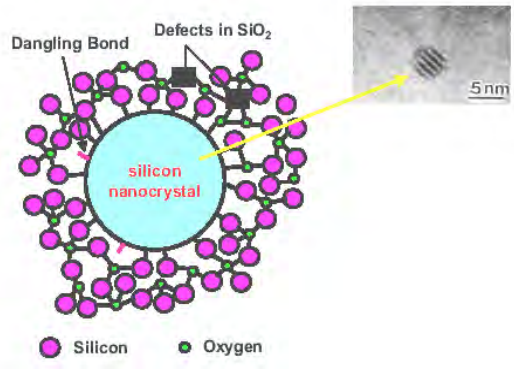

Figure 3.3: *Silicon nanocrystals embedded in SiO_2.*

on photoluminescence intensity.

We formulate a model for photoluminescence intensity by taking the effect of surface and exciton states into account in the coming section. In addition, we give a quantitative expression for the photoluminescence intensity.

3.2 Formulation of a model to generate photoluminescence spectra

The study of silicon quantum dot is a very active field of research due to the interesting fundamental physical properties and the promising applications in advanced electronic and optoelectronic devices [10]. The optical properties have studied intensively for frequencies near the fundamental energy gap of the dots with respect to photoluminescence. Here we are going to formulate and describe the photoluminescence spectra from silicon quantum dot. To do so, let us consider silicon quantum dots as an ensemble of having a well defined size distribution function $n(d)$.

On excitation with high-energy photons, photocarriers have generated inside the crystals and then a fraction of these photoexited carriers relax non - radiatively to the surface states. Subsequently, the relaxed carriers recombine to ground states radiatively giving photoluminescence. So, the intensity of photoluminescence at particular

photon energy becomes proportional to the population of occupied surface states and the oscillator strength. The number of surface states N_s in a quantum dots is proportional to the number of atoms on the surface and hence, surface area A of the quantum dot. Additionally, if we assume that each atom in a quantum dots contributes at least one photoexited carrier, the number of photoexited carriers N_v in the quantum dots are proportional to volume V.

The rate of transition from an excited carrier to the localized surface states is proportional to the product of the number of excited photocarriers and the number of available empty surface states in steady state condition, the population N_r of photocarriers in surface states participating in photoluminescence processes becomes proportional to the product, i.e.

$$N_r \sim A\ V \tag{3.2.1}$$

For a quantum dots of diameter d we have $V \sim d^3$ and $A \sim d^2$. So we get

$$N_r \sim d^5 \tag{3.2.2}$$

In the strong confinement regime, blue shift in band gap energy is quite significant compared to weak confinement limit. Along with the blue shift of the band gap and excitonic levels, particle size reduction also causes an enhancement in the oscillator strengths (f). That is, optical transition probability in a bulk semiconductor is proportional to the probability of finding an electron and a hole in the same unit cell of the crystal. Hence, the oscillator strength of the exciton, f_{ex}, is inversely proportional to a_B^3. In the case of quantum dots transition probability is proportional to the spatial restriction of carrier motion in the quantum dots volume due to externally imposed quantum confinement [15], i.e.

$$f \sim \frac{1}{d^3}$$

Now, taking the oscillator strength into account, the radiative transition probability in a quantum dots of diameter d becomes

$$P(d) \sim f\, N_r \sim d^2 \tag{3.2.3}$$

Now, the photoluminescence intensity from an ensemble of quantum dots size d having size distribution n(d) will be given by

$$I(d) \sim P(d)\ n(d) \tag{3.2.4}$$

The emitted photon energy from the quantum dots should be lower than the band gap energy of quantum confinement model by an amount of the localization binding energy E_s of the surface states and the exciton binding energy E_b. Hence, the emitted photon energy from quantum dots will be

$$E_{pl} = E_g^{bulk} + \triangle E - E_b - E_s \tag{3.2.5}$$

According to quantum confinement model, the band gap up shift modeled as $\triangle E = \frac{\beta}{d^\gamma}$, where β and γ are constants due to quantum confinement effect, their magnitudes strongly depend up on the band gap calculation method being employed. We transform Eq. 3.0.6 from d to $\triangle E$ dependence [20] as

$$I(\triangle E) = \int I(d)\ n(d)\delta(\triangle E - \frac{\beta}{d^\gamma})\ d\ d \tag{3.2.6}$$

taking

$$n(d) = \frac{1}{\sigma\sqrt{2\pi}} exp(-\frac{(d-d_o)^2}{2\sigma^2})$$

Where d_o and σ are the mean dot size and standard deviation respectively. Therefore, we obtained an expression for the photoluminescence intensity as

$$I(\triangle E) \sim \frac{1}{\sigma\sqrt{2\pi}}(\frac{\beta}{\triangle E})^{\frac{2}{\gamma}} exp[-\frac{\{(\frac{\beta}{\triangle E})^{\frac{1}{\gamma}} - d_o\}^2}{2\sigma^2}] \tag{3.2.7}$$

Eq. 3.0.9 gives general expression for photoluminescence intensity from silicon quantum dots ensemble. It is clear from the above expression is that the photoluminescence intensity depends strongly on the quantum confinement parameters β and γ. We took $\gamma = 1.39$, $\beta = 3.73\ eV$ and $E_g^{bulk} = 1.12\ eV$ at room temperature [5]. The localization binding energy E_s has taken to be the order of phonon energies, which is about 0.05 eV for optical phonons.

It is important to note that earlier researchers have taken oscillator strength as proportional to $\frac{1}{d^\alpha}$ but we used $\frac{1}{d^3}$. Now, we use eqn. 3.2.9 along with exciton contribution to generate photoluminescence spectra for different size of quantum dots using MATLAB programming (added as appendices). We then compare our result derived from the model with the experimental and simulation results of others.

Chapter 4

Results and discussions

Together with Silicon nanocrystals, silicon nanowires used to model the optical and photoluminescence properties of porus and crystalline silicon. However, despite the large amount of experimental data available, Mruno *et al.* 's [21] understanding of the electronic properties of silicon nanowires and porus silicon is almost confined to single-particle calculations done with semiempirical methods or with the *ab initio* density functional theory (DFT), usually within the local density approximation (LDA).

In Fig. 4.1 (a) Mruno *et al.* compare the quasiparticle electronic gaps with the experimental data obtained by Ma *et al.* through scanning tunneling spectroscopy, for different silicon nanowires (grown along the [112] and [110] directions) with diameters ranging from 1.3 to 7 nm and shown in Fig. 4.1 (b), they also compared the silicon nanowires quasiparticle with the experimental photoluminescence gaps of porus silicon, they observed that the quasiparticle gaps largely overestimate the experiment. Here, we mentioned this results since researchers are recently trying to broad their field of study towards quantum wire some what to quantum well than quantum dots but our study deals about quantum dots, anyhow from such results we understood that the optical band gap of silicon quantum wire and quantum dots are almost have the same variation as the crystal size decreases specially less than 5 nm in diameter.

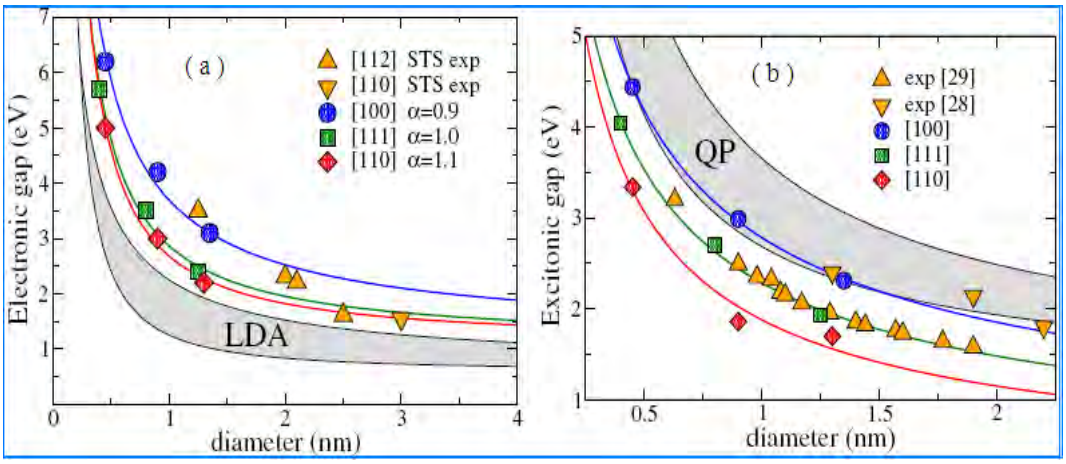

Figure 4.1: *a) (Color online) QP gaps for [100] (circles), [111] (squares), and [110] (diamonds) Si-NWs as a function of wire size compared with experimental results (triangles) from scanning tunneling spectroscopy (STS). The gray region represents the LDA electronic gaps from [110] (bottom) to [100] (top) wires. b) (Color online). Excitonic gaps for [100] (circles), [111] (squares), [110] (diamonds) Si-NWs, and experiments (triangles). Down- and up-pointing triangles correspond, respectively, to the photoluminescence data of Zhang and Bayliss and Wolkin* et al. *in PS samples. The gray region represents the quasiparticle electronic gaps, from [110] (bottom) to [100] (top) wires.*

4.1 Results of optical band gap when exciton states are taken into account

In experimental work carried out over the past two decades on silicon nanocrystals, the optical band gap dependence on the dots size measured and discussed extensively. Some of such experimental works result presented together with our models result for the sake of comparison in figure 4.2.

In fact, there is a large spread in the calculated values of the optical band gaps as a function of nanocrystals diameter. Among several factors influencing the accuracy of the optical band gap measurements, the following are dominant [2]. First, it is difficult to determine exactly the dot sizes and the size distribution in a luminescent ensemble

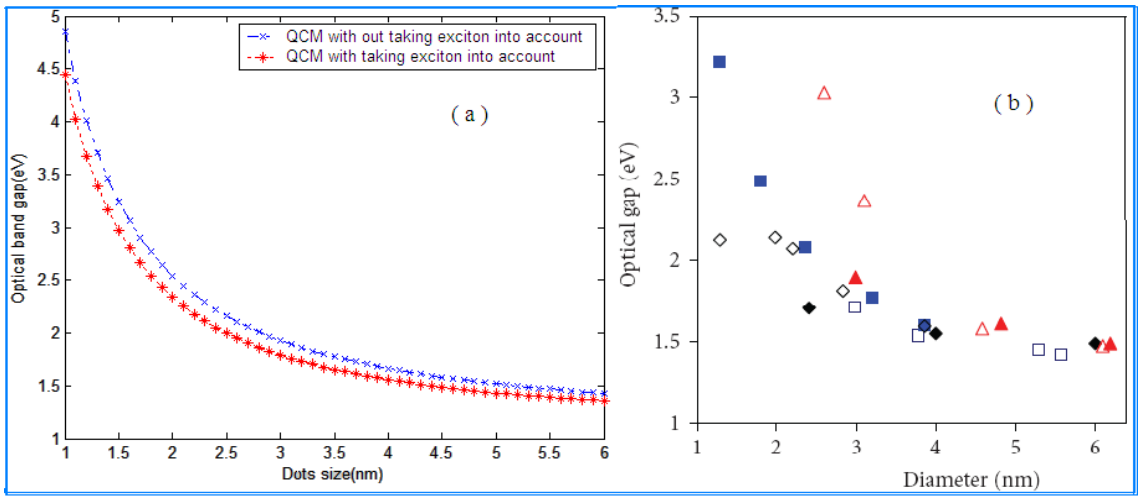

Figure 4.2: *a) Size dependence of silicon quantum dots band gap, according to QCM with and without taking exciton into account (our result). b) Experimental data on the size dependence of the optical gap of silicon crystals. Hydrogen - passivated surface Wolkin* et al. *and Garrido* et al. *(blue squares); SiO - bonds at the surface Wolkin* et al., *Kanemitsu* et al. *(diamonds); deposition on quartz substrate Ledoux* et al. *(filled triangles); nanocrystals embedded in Si_3N_4 matrix Kim* et al. *(empty triangles) [2].*

of nanocrystals. Second, using the mean size in an ensemble of nanocrystals in a diagram, as Figure 4.2 (b) can be misleading. Since, it is possible that the observed photoluminescence peak does not correspond exactly to the mean size but instead to the largest photoluminescence rate. Third and more practically, the nanocrystal studied by different research groups have prepared by different methods. As a result, the nanocrystals have different surroundings, surface bonds, and shapes, all of which could lead to scatter in the experimental data and nanocrystal-nanocrystal interactions can play a dominant role in the emission spectrum.

When we compare our plot by taking exciton effect along with quantum confinement model (figure 4.2 (a)) explains almost accurately the Wolkin *et al.* and Garrido *et al.* (blue squares) experimental data. Therefore, taking the appearance of exciton energy

states, band of exciton energy levels, in the forbidden region into account leads to a better explanation, even if the above constraints did not allow us to predict the exact theoretical explanations.

4.2 Results of photoluminescence intensity when exciton states are taken into account

4.2.1 Photoluminescence intensity versus dot size

Different experiments have performed on Silicon nanocrystals to see the effect of quantum confinement and surface states. Figures 4.3 and 4.4 shows the photoluminescence spectra of different samples studied with their size distributions as measured by time-of-flight mass spectroscopy (TOFMS) together with results of our model i.e. normalized photoluminescence intensity versus dots size, for experimental and results of our model for two set of samples.

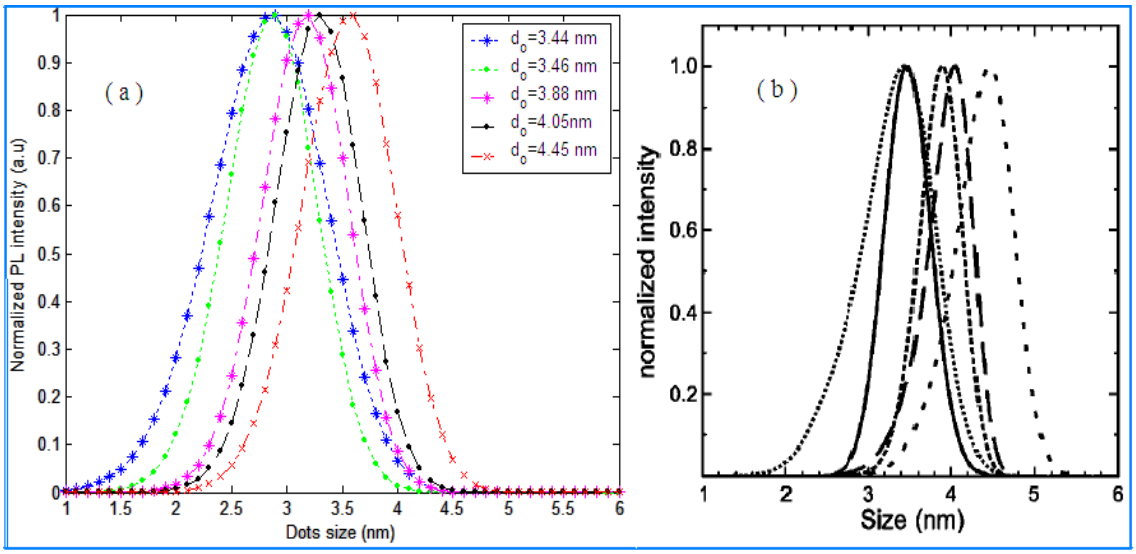

Figure 4.3: *Normalized PL intensity versus dot size for the first set of samples. a) Results of our model b)Experimental [22].*

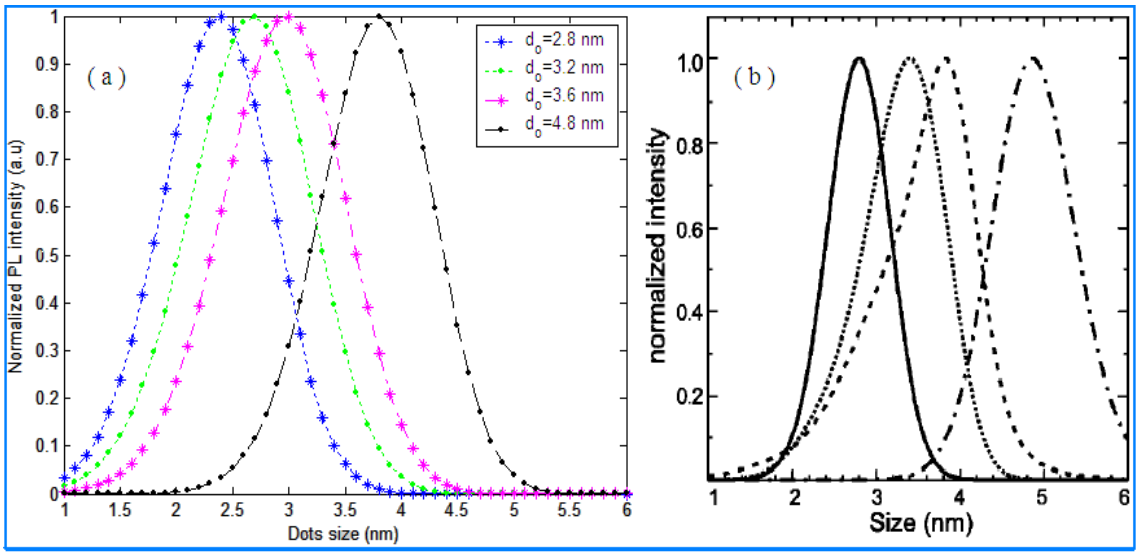

Figure 4.4: *Normalized PL intensity versus dot size for the second set of samples. a) Results of our model b) Experimental [22].*

When we looked at those pictures, we realized that the photoluminescence peak shifts towards left or to the smaller wavelength of visible spectrum (blue shifted) as the dots size decreases, which is expected. Researchers' understood that width of size distribution and the average size of quantum dots are realities that cause such shifts. We also find out that the existence of exciton states in the forbidden region have remarkable effects for such shifts. Therefore, taking the formation of band of exciton energy states in the band gap into account leads to the accurate formulation of photoluminescence spectra and the interpretation of the blue shift of photoluminescence peak especially when the quantum dots size less than 2 nm in conformity with different experimental and theoretical results. Note that the data we took from G. Ledoux *et al.* (2000) [22] research work i.e. the maximum positions and the bandwidths and our data are reported in table 4.1 and 4.2 respectively for the sake of comparison.

Sample identifier	Average size (nm)	Width of size distribution(nm)	PL Max. (eV)	PL Max. (nm)	PL width (nm)
A	3.44	1.02	1.82	680	190
B	3.46	0.63	2.03	610	165
C	3.88	0.61	1.75	710	155
D	4.05	0.62	1.65	750	150
E	4.45	0.78	1.55	800	145
K	2.8	0.86	1.95	635	115
L	3.2	1.08	1.71	725	145
M	3.6	1.16	~1.44[a]	~860[a]	~170[a]
N	4.8	1.16	1.35[a]	900[a]	~200[a]

a- values derived from Gaussion fits to the experimental data

Table 4.1: *Characteristic parameters and PL properties of the different silicon nanocrystal samples studied [22].*

Sample identifier	Average size (nm)	PL Max. (eV) Experimental	PL Max. (eV) results of our model	PL Max. (nm) Experimental	PL Max. (nm) results of our model
A	3.44	1.82	1.6178	680	728.496
B	3.46	2.03	1.6131	610	730.728
C	3.88	1.75	1.5278	710	773.774
D	4.05	1.65	1.4993	750	789.339
E	4.45	1.55	1.4427	800	822.318
K	2.8	1.95	1.8130	635	646.965
L	3.2	1.71	1.6799	725	700.352
M	3.6	1.44	1.5919	860	745.848
N	4.8	1.35	1.4025	900	847.613

Table 4.2: *Our model's results as compared with PL properties of different silicon nanocrystal samples.*

4.2.2 Photoluminescence intensity versus wavelength

Just like former section, figures 4.5 and 4.6 shows the photoluminescence spectra of different samples studied with their size distributions as measured by time-of-flight mass spectroscopy (TOFMS) together with results of our model. From such plots, we understood that as the average size of the sample decreases the optical band gap increases so that the photoluminescence peak shifts to the shorter wavelength range of visible spectrum. Since, the luminescence energy is directly proportional to the

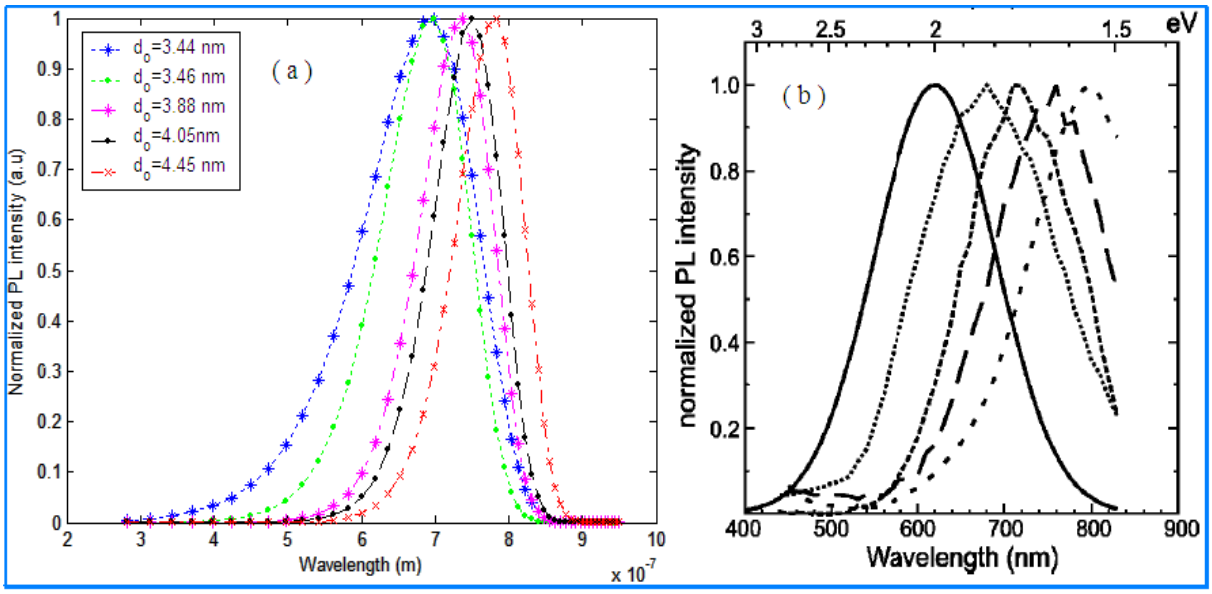

Figure 4.5: *Normalized PL intensity versus wavelength for the first set of samples a) Results of our model b) Experimental [22].*

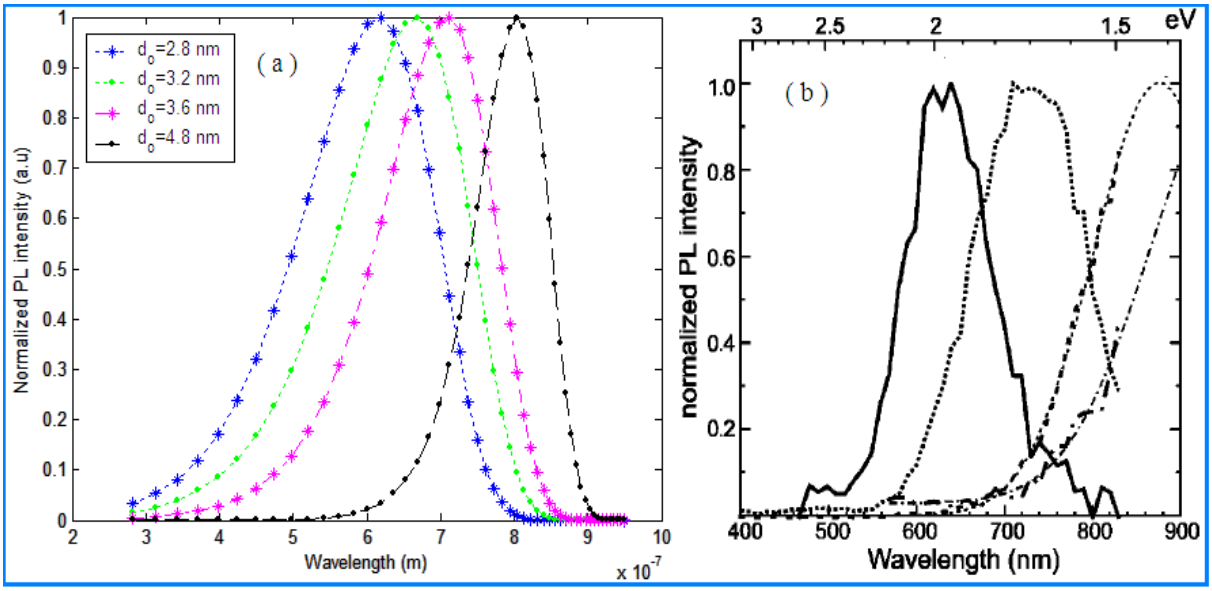

Figure 4.6: *Normalized PL intensity versus wavelength for the second set of samples a) Results of our model b) Experimental [22].*

optical band gap and inversely proportional to wavelength. Therefore, as the optical band gap increases the luminescence energy increases or wavelength decreases mostly to the shortest wavelength of visible spectrum. However, when exciton effects taken into account i.e. the theory we developed by considering the band of exciton energy states in the band gap explains the experimental data better than without taking such band of states.

Here it is important to note that the exciton binding energy (E_b) is the energy width of strongly confined exciton, band width of strongly confined exciton energy states, since the average size of our samples are less than 5 nm ($d \leq a_B$).

Chapter 5

Summary and conclusion

5.1 Summary

The study of silicon nanostructures (quantum dots) is a very active field of research because of the strong room temperature photoluminescence and the observation of quantum size effects. Nanostracturing silicon is also an effective way to turn silicon into a photonic material since as different experimental and theoretical predictions indicated that the indirect band gap of bulk silicon changed in to direct band gap and the optical band gap increases as the crystal size decreases (especially when it reaches few nanometer size). When an electron in the valance band of such quantum dots gets sufficient photon energy excites and leaves a hole behind then the excited electron gate couple with the corresponding hole such pair is said to be an exciton and creates energy states in the forbidden region. For repeated such excitation the number of exciton states in the gap region increases and form little band. Such band of energy states in the band gap act as an alternative destination for an electron excites from the valance band. Hence, the existences of such states in the forbidden region have their own effects on optical band gap and consequently on all physical

properties of silicon quantum dots and their effects observed as a blue shift in the photoluminescence peak.

To realize the effect of such band of exciton energy states on the band gap and other properties, we analytically expressed the photoluminescence intensity by taking the appearance of such exciton energy states in the band gap into account in addition to surface states and quantum confinement effects in order to describe the experimental photoluminescence spectra from silicon quantum dots. Accordingly, we observed that taking such band of states in the band gap lead to a better theoretical explanation of the photoluminescence data from different experimental techniques.

5.2 Conclusion

Recent studies show that the density of states of silicon nanostructures is atomic like rather than bulk. This discrete structure in the density of states has direct link with the exciton energy. The exciton energy levels modify the band structure of nanosystems. As a result, the optical properties also modified. At lower temperature, these effects become more prominent. Due to the contribution of exciton the electroluminescence and photoluminescence spectra shows sharp peak with small kinks. As the size of the quantum dots decreases the effect, become more robust. Our observation is in agreement with many experimental and theoretical observations [23] - [25].

Based on our study, taking the effect of the existence of exciton energy states in the forbidden region on optical band gap describes better the experimental photoluminescence data from silicon quantum dots developed by several experimental techniques. Therefore, our study shows that the importance of exciton energy levels in predicting

the photoluminescence data from silicon quantum dots using quantum confinement and surface state models together. Hence, the result we obtained could apply for controlled light emitting properties in photonic material production.

Here we have looked at room temperature photoluminescence for silicon quantum dots. Temperature dependent optical behavior with surface passivation for different nanostructures is worth to look at. Our model is quite general phenomenological model in which temperature dependence be incorporated.

Appendices

It is important to note that when we plot the graphs, we used the following numerical data.

- $m_o \ = \ 9.11 \ \times \ 10^{-31} \ Kg$
- $h \ = \ 4.136 \ \times \ 10^{-15} \ eV \ s$
- $c \ = \ 2.998 \ \times \ 10^{8} \ m/s$
- $\varepsilon_r \ = \ 11.68$
- $\varepsilon_0 \ = \ 8.854 \ \times \ 10^{-12} \ F \ m^{-1}$
- $m_e^* \ = \ 0.40 \ m_o$
- $m_h^* \ = \ 0.54 \ m_o$
- $a_H \ = \ 0.05292 \ nm$
- $E_{RY}^* \ = \ \frac{\mu}{m_o} \ \frac{1}{\varepsilon_r^2} \ \times \ 13.6 \ eV \ = \ 0.0229 \ eV$

A : *A MATLAB program to plot optical band gap Vs size*

$d = 1 : 0.15 : 8$

$eg1 = 1.12 + 3.73./(d.\hat{} \ 1.39)$

$eg2 = 1.12 + 3.73./(d.\hat{} \ 1.39) - 0.2./(d./2) - 0.005679$

$plot \ (d, \ eg1, \ 'r : o', \ d, \ eg2, \ 'b - .*')$

$legend \ ('QCM \ with \ out \ taking \ exciton \ into \ account', \ 'QCM \ with \ taking$

$exciton\ into\ account')$

$xlabel\ ('Dots\ size\ (\ nm)'),\ ylabel\ ('Band\ gap\ (\ eV)')$

B : *A MATLAB program to plot normalized photoluminescence intensity versus size of the first group* $(A\ -\ E)$

$d = 1 : 0.15 : 6$

$de = 3.73./(d.\hat{}\ ^{1.39}) - 0.2./(d./2) - 0.055679$

$ia = exp\ (-(((3.73./de).\hat{}\ ^{0.7194} - 3.44).\hat{}\ ^{2})./1.02)$

$ib = exp\ (-(((3.73./de).\hat{}\ ^{0.7194} - 3.46).\hat{}\ ^{2})./0.63)$

$ic = exp\ (-(((3.73./de).\hat{}\ ^{0.7194} - 3.88).\hat{}\ ^{2})./0.61)$

$id = exp\ (-(((3.73./de).\hat{}\ ^{0.7194} - 4.05).\hat{}\ ^{2})./0.62)$

$ie = exp\ (-(((3.73./de).\hat{}\ ^{0.7194} - 4.45).\hat{}\ ^{2})./0.78)$

$plot\ (d,\ ia,\ 'r : *',\ d,\ ib,\ 'b : .',\ d,\ ic,\ 'g - .*',\ d,\ id,\ 'k - -.',\ d,\ ie,\ 'm - .x')$

$legend\ ('d_o = 3.44\ nm',\ 'd_o = 3.46\ nm',\ 'd_o = 3.88\ nm',\ 'd_o = 4.05\ nm',\ 'd_o = 4.45\ nm')$

$xlabel\ ('Dots\ size\ (nm)'),\ ylabel\ ('Normalized\ PL\ intensity\ (a.u)')$

C : *A MATLAB program to plot normalized photoluminescence intensity versus size of the second group* $(K\ -\ N)$

$d = 1 : 0.15 : 6$

$de = 3.73./(d.\hat{}\ ^{1.39}) - 0.2./(d./2) - 0.055679$

$ik = exp\ (-(((3.73./de).\hat{}\ ^{0.7194} - 2.8).\hat{}\ ^{2})./0.86)$

$il = exp\ (-(((3.73./de).\hat{}\ ^{0.7194} - 3.2).\hat{}\ ^{2})./1.08)$

$im = exp\ (-(((3.73./de).\hat{}\ ^{0.7194} - 3.6).\hat{}\ ^{2})./1.16)$

$in = exp\ (-(((3.73./de).\hat{}\ ^{0.7194} - 4.8).\hat{}\ ^{2})./1.16)$

$plot\ (d,\ ik,\ 'r : *',\ d,\ il,\ 'b : .',\ d,\ im,\ 'g - .*',\ d,\ in,\ 'k - -.')$

$legend\ ('d_o = 2.8\ nm',\ 'd_o = 3.2\ nm',\ 'd_o = 3.6\ nm',\ 'd_o = 4.8\ nm')$

$xlabel\ ('Dots\ size\ (\ nm)'),\ ylabel\ ('Normalized\ PL\ intensity\ (a.u)')$

D : *A MATLAB program to plot normalized photoluminescence intensity versus wave length of the first group* $(A - E)$

$d = 1 : 0.15 : 6$

$de = 3.73./(d.\hat{}\ ^{1.39}) - 0.2./(d./2) - 0.055679$

$el = 1.12 + 3.73./(d.\hat{}\ ^{1.39}) - 0.2./(d./2) - 0.055679$

$l = 1239.931e - 9./el$

$ia = exp\ (-(((3.73./de).\hat{}\ ^{0.7194} - 3.44).\hat{}\ ^{2})./1.02)$

$ib = exp\ (-(((3.73./de).\hat{}\ ^{0.7194} - 3.46).\hat{}\ ^{2})./0.63)$

$ic = exp\ (-(((3.73./de).\hat{}\ ^{0.7194} - 3.88).\hat{}\ ^{2})./0.61)$

$id = exp\ (-(((3.73./de).\hat{}\ ^{0.7194} - 4.05).\hat{}\ ^{2})./0.62)$

$ie = exp\ (-(((3.73./de).\hat{}\ ^{0.7194} - 4.45).\hat{}\ ^{2})./0.78)$

$plot\ (l,\ ia,\ 'r : *',\ l,\ ib,\ 'b : .',\ l,\ ic,\ 'g - .*',\ l,\ id, ''k - -.',\ l,\ ie,\ 'm - .x')$

$legend\ ('d_o = 3.44\ nm',\ 'd_o = 3.46\ nm',\ 'd_o = 3.88\ nm','d_o = 4.05\ nm',\ 'd_o = 4.45\ nm')$

$xlabel\ ('Wave\ length\ (\ m)'),\ ylabel('Normalized\ PL\ intensity\ (a.u)')$

E : *A MATLAB program to plot normalized photoluminescence intensity versus wave length of the second group* $(K - N)$

$d = 1 : 0.15 : 6$

$de = 3.73./(d.\hat{}\ ^{1.39}) - 0.2./(d./2) - 0.055679$

$el = 1.12 + 3.73./(d.\hat{}\ ^{1.39}) - 0.2./d - 0.055679$

$l = 1239.931e - 9./el$

$ik = exp\ (-(((3.73./de).\hat{}\ ^{0.7194} - 2.8).\hat{}\ ^{2})./0.86)$

$il = exp\ (-(((3.73./de).\hat{}\ ^{0.7194} - 3.2).\hat{}\ ^{2})./1.08)$

$im = exp\ (-(((3.73./de).\hat{}\ ^{0.7194} - 3.6).\hat{}\ ^{2})./1.16)$

$in = exp\ (-(((3.73./de).\hat{}\ ^{0.7194} - 4.8).\hat{}\ ^{2})./1.16)$

$plot\ (l,\ ik,\ 'r : *',\ l,\ il, ''b : .',\ l,\ im,\ 'g - .*',\ l,\ in,\ 'k - -.')$

$legend\ ('d_o = 2.8\ nm',\ 'd_o = 3.2\ nm',\ 'd_o = 3.6\ nm',\ 'd_o = 4.8\ nm')$

$xlabel\ ('Wave\ length\ (\ m)'),\ ylabel\ ('Normalized\ PL\ intensity\ (a.u)')$

Glossary

- 2D-PC - Two - dimensional photonic crystal
- AFM - Atomic Force Microscopy
- CB - Conduction Band
- DFT - Density Function Theory
- EL - Electroluminescence
- EMA - Effective mass approximation
- HOMO - Highest occupied molecular orbital
- LDA - Local Density Approximation
- LED - Light Emitting Diode
- LUMO - Lowest unoccupied molecular orbital
- NC -Nano-Crystalline
- NW - Nanowire
- PL -Photoluminescence
- PSi - Porous Silicon
- QCM - Quantum Confinement Model

- QD - Quantum Dot
- QP - Quasiparticle
- STS - Scanning tunneling spectroscopy
- TOFMS - Time - of - flight mass spectroscopy
- VB - Valence Band
- QCM - Quantum Confinement Model

Bibliography

[1] http://en.wikipedia.org/wiki/Main-Page (Accessed on August 3, 2008).

[2] V. A. Belyakov, V. A. Burdov, R. Lockwood, and A.Meldrum, Adv. Opt. Tech., **ID279502**, 32 (2008).

[3] H. Takagi H. Ogawa, Y. Yamaziki, A. Ishizaki and T. Nakagiri, Appl. Phys. Lett., **56**, 24 (1990).

[4] V.A. Fonoberov and E.P. Pokatilov, Phys. Rev. B, **66**, 085310 (2002).

[5] J.P. Proot, C. Delerue and G. Allan, Appl. Phys. Lett., **61**, 16 (1992).

[6] S. Tripathy, R.K. Soni, S.K. Ghoshal and K.P. Jain, Bull. Mater. Sci., **24**, 3 (2001).

[7] Karl W. Böer, *Survey of Semiconductor Physics: Electrons and Other Particles in Bulk Semiconductors*, Nostrand Reinhold, 1990.

[8] H. Ch. Weissker, J. Furthmüller and F. Bechstedt, Phys. Rev. B, **65**, 155327 (2002).

[9] H. Ch. Weissker, J. Furthmüller and F. Bechstedt, Phys. Rev. B, **65**, 155328 (2002).

[10] S. K. Ghoshal, Devendara Mohan, Tadesse Tenaw Kassa and Sunita Sharma, Int. J. Mod. Phys. B, **21**, 22, (2007).

[11] L. Pavesi, Adv. Opt. Tech., **ID416926**, 12 (2008).

[12] C. Delrue, G. Allan and M. Lannoo, Phys. Rev. B, **48**, 15 (1993).

[13] Robert Joseph Walters, Ph.d Thesis, *Silicon Nanocrystals for Silicon Photonics*, California Institute of Technology, Pasadena, California (2007).

[14] Y. Kayannuma and H. Momiji, Phys. Rev. B, **41**, 14 (1990).

[15] B.P. Singh, Bull. Mater. Sci. **29**, 6 (2006).

[16] G Rajagopal and Paul Wright, *Quantum Confinement Effects in Semiconductor Clusters*, Churchill College, Cambridge (2000), internet article.

[17] M. V. Wolkin, J. Jorne and P.M. Fauchet, Phys. Rev. Lett., **82**, 1 (1999).

[18] Shuji Hasegawa, J. Phys.: Cond. Matt. **12**, R463 (2000).

[19] Zhiyong Zhou, Michael L. Steigerwald, Richard A. Friesner, Louis Brus and Mark S. Hybertsen, Phys. Rev. B, **71**, 245308 (2005).

[20] V. Ranjan and Vijay A. Singh, Phys. Rev. B, **58**, 3 (1998).

[21] M. Bruno, Maurizia Palummo, Andrea Marini, Rodolfo Del Sole, and Stefano Ossicini, Phys. Rev. Lett., **98**, 036807 (2007).

[22] G.Ledoux, O. Guillois, D. Porterat and C. Reynaud, Phys. Rev. B, **62**, 23 (2000).

[23] L. Tsybeskov, E. K. Lee, H. Y. Chang, B. V. Kamenev, D. J. Lockwood, J. M. Baribeau, and T. I. Kamins, Adv. Opt. Tech., **ID218032**, 10 (2008).

[24] Eleonora Luppi, Federico Iori, Rita Magri, Olivia Pulci, Stefano Ossicini, Elena Degoli, Valerio Olevano, Phys. Rev. B, **75**, 033303 (2007).

[25] F. Trani, F. Trani, D. Ninno and G. Iadonisi, Phys. Rev. B, **75**, 033312 (2007).

[26] S.K. Ghoshal, Ashagrie Mekuriaw, M.Sc thesis, *Nanosilicon for Optoelectronic Application. A Model to Study Photoluminescence*, Addis Ababa University, Addis Ababa, Ethiopia (2008).

DECLARATION

I hereby declare you that this thesis is my original work, has not been presented for a degree in any other Universities and has been presented with the help of my advisor and instructor. All sources of material used for the thesis have been duly acknowledged.

Name: *Tesfaye Shiferaw Haile*

Signature: .....

This thesis has been submitted for the examination with my approval as university advisor.

Name: Dr. S. K. Ghoshal

Signature: .....

Addis Ababa University
Department of Physics
June, 2009